TM-785
1670.000

Fermilab

# THE DESIGN OF THE BEAM TRANSFER SYSTEM FOR THE DOUBLER SECTOR TEST

M. Harrison

April 18, 1978

## Summary

In this report we shall describe the design and major operational characteristics of the sector test transfer system. An outline of the design philosophy will be presented as well as an analysis of the orbit sensitivity with respect to such parameters as tune instability, momentum dispertion and consequences of replacing main ring elements with similar but non-identical elements in the sector.

## Introduction

The sector test was originally constructed as an in situ, and as far as possible, realistic test of associated hardware. The test itself, as first conceived by Tom Collins, calls for the establishment of a 100 GeV coasting beam in the Main Ring which would then be diverted, using a fast one-turn kicker, on to a new stable circulating orbit passing through 5/6 of the Main Ring and 1/6 of the Doubler. The 1/6 sector of the Doubler ring is positioned beneath section A of the Main Ring. Entrance to and exit from the sector is effected via vertically bending Lambertson magnets positioned in the Main Ring at the A0 and B0 straight sections.

Before launching into the details of a realistic beam transfer system, a simple explanation of the basic principles involved in this machine bypass operation may lend some clarity to the rest of this report. As stated above, two stable equilibrium orbits are required with the transistion between the first (Main Ring equilibrium orbit) and the second (sector test equilibrium orbit) achieved by a single turn horizontal kicker located in the Main Ring.

If we consider the Main Ring as the "ideal" machine (perfect magnet alignment, no sextupole or higher order magnet fields) then the circulating beam would lie on a smooth orbit passing through the centre of each element in the ring (the so-called equilibrium orbit). From the point of view of this Main Ring it is sufficient to describe the sector bypass by two apertures, an entrance and an exit, and the remark that no beam is lost in the sector. The internal dynamics of the sector are, as yet, undefined. A beam passing through the sector apertures is, of necessity, displaced from the Main Ring equilibrium orbit, and as such if not corrected by any steering will execute betatron oscillations around the Main Ring equilibrium orbit. The situation of an orbit passing through the sector can be represented schematically as follows:

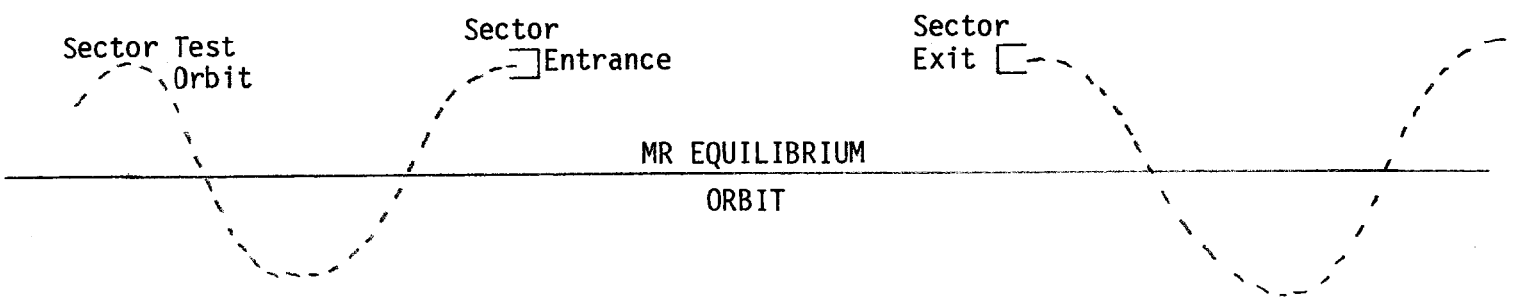


If the sector test orbit is to be stable (a stable orbit is an orbit which returns to the same position after each revolution) with maximum orbit excursions at both the entrance and exit to the sector then this orbit in the Main Ring must perform an integral number of betatron oscillations. The requirement of maximum orbit excursions at the sector-apertures is equivalent to minimizing the amplitude of the betatron oscillations in the Main Ring needed to establish the sector orbit. The number of oscillations in the Main Ring is a machine parameter governed primarily by the quadrupole field strength. The conventional way to describe these oscillations is in terms of phase advance normalized to $2\pi$, hence we can say the sector orbit requires an integral phase advance from the sector exit to the sector entrance.

So far we have mentioned the equilibrium orbit in the Main Ring and the stable orbit through the sector without describing the transistion between the two. This operation is accomplished by using a kicker magnet to provide the suitable angular deflection to move the beam from the Main Ring equilibrium orbit onto the sector test orbit. It is apparent that this orbit switch can only be made at those certain positions in the Main Ring where both orbits intersect, thus:

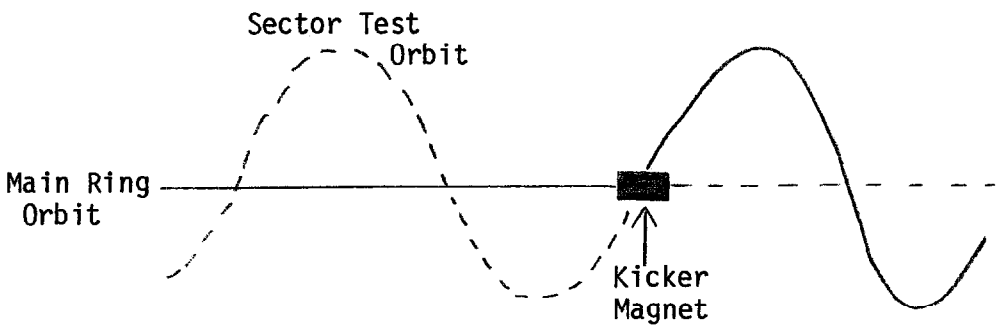


The establishment of a stable sector orbit, can therefore be thought of as imposing certain basic conditions on the machine operation. The rest of this report will attempt to establish and investigate these conditions.

In the currently proposed sector test the so-called entrance and exit to the sector are Lambertson magnets located ∿20 ms upstream from A0 and downstream from B0. An integral phase advance between these two points suggests a horizontal machine tune of 19.31 as opposed to the "normal" machine tune of 19.4, (the machine tune is defined as the total phase advance through one complete evolution) as the operational tune for the sector test. Unless specifically stated a machine tune of 19.31 has been used in all orbit calculations.

Beam Transfer System

One turn extraction from the Main Ring is accomplished by using horizontal pulsed kicker magnets (∿350 ns rise time) to move the Main Ring beam from the stable orbit position across the thin septum in the Lambertson magnets and into their dipole field region. Once inside this dipole field the beam is deflected down from the Main Ring and towards the Doubler sector. In order to minimize the magnitude of the kick needed to move the Main Ring beam across the Lambertson septum, pairs of bump magnets are used to induce horizontal local orbit distortions bringing the beam close to the septum before injection into the sector. Appendix I gives a brief description of such localized deflecting systems. For the purposes of this test these local orbit distortions are induced by pairs of bump magnets in the Main Ring at F46-A17 and A42-B13. Each pair possessing a relative phase difference of 0.9635. Figure 1 shows both pairs of bump magnets producing local orbit distortions in the vicinity of the Lambertson magnets.

In order to achieve sufficient downward bend in the A0 straight section to drop the beam 63.5 cms into the sector, two Lambertson magnets are needed starting ∿20 ms upstream of A0 giving a combined bend of 15 mrad. Extraction from the sector requires a reciprocal pair of magnets ∿20 ms downstream of B0.

To achieve a vertically flat orbit through the sector one EPB dipole and a smaller trim dipole are needed to remove the 15 mrad vertical bend. These two magnets are located some 21 m downstream from A0, with a similar pair 21 m upstream of B0 starting the extraction bend back up to the Main Ring. Two more small vertical dipoles placed just upstream from A12 and just downstream from A48 allow up to 800 μr of vertical steering through the sector. To obtain a horizontally smooth orbit through the sector two horizontal bump magnets located

at A12 and A47 are required to smooth out the betatron oscillations induced by the kicker magnet as well as the local orbit distortions from the Main Ring bump magnets at F46 and B13. (The beam is now passing through the sector and as such will not be affected by the A17, A42 Main Ring bump magnets.) The relative phase change across the "new" pairs of bump magnets is 0.5023.

An example of a closed orbit which is smooth through the sector is shown in Fig. 2. The large betatron oscillations in the Main Ring are due to the fact that a $\sim$2.0 cm difference in radial offset is required at the Lambertson magnet, between the closed orbit through the Main Ring and the closed orbit in the Main Ring plus sector. This extra 2.0 cm represents the minimum displacement needed to move the beam across the Lambertson septum. Figure 3 shows the different beam positions at the upstream end of the A0 Lambertsons.

The relative amplitude and phase between two closed orbits generally precludes the use of just one pulsed kicker magnet to make the transition between the two. For the purposes of the sector test we will use the existing extraction kicker magnet at C48 together with a small orbit correcting kicker at D48. Figure 4 shows schematically the two kicker magnets accomplishing the transition between the closed orbit in the Main Ring (Fig. 1) and the sector test orbit (Fig. 2).

Table I gives a list of the transfer system elements together with their position and bend angles. Figures 5 and 6 give a schematic representation of these elements with respect to the upstream and downstream ends of the sector.

Figure 7 shows a closed orbit solution through the sector optimized for a machine tune of 19.4. A machine tune of this value gives a phase advance of 16.065 in the Main Ring as opposed to 15.995 obtained with a 19.31 tune. Comparing this with Fig. 2 gives an indication of the advantage of using a 19.31 machine tune to provide a smooth orbit in the sector.

A stable orbit, such as that shown in Fig. 2 has large betatron oscillations ($\sim\pm3.5$ cms) in the Main Ring. The size of these oscillations brings the beam uncomfortably close to the limiting Main Ring aperture. The magnitude of these oscillations can be reduced by a technique of mismatching the local bump magnets prior to the extraction kick. An appropriate mismatch of the Main Ring bump magnets can be found which will set up a long equilibrium orbit bump of 15-1/2 oscillations between B13 and F46 in the Main Ring which is out of phase with the sector test orbit as shown in Fig. 2, and about 1/2 its amplitude. Under these new conditions the affect of the kicker magnet when changing orbits will be to reverse the phase of the orbit distortion between B13 and F46, the amplitude of the distortion will be about 1/2 of that shown in Fig. 2. This substantial reduction in orbit displacement is demonstrated in Figs. 8, 9 and 10. Here we start again from Fig. 1 with equal currents in the bump magnets at F46-A17 and different but equal currents in A42 and B13. Figure 8 shows the Main Ring orbit generated by changing the currents in F46 and B13 bumps by equal amounts. Comparing this with Fig. 1 we can see that the orbit displacement at the Lambertson septa is unchanged.

Figure 9 shows the kicker magnets changing the phase of the oscillations. Figure 10 then shows these smaller oscillations with the correct phase reinforcing the bump magnets to produce a sufficient orbit displacement at the Lambertsons to enter the sector. Comparing Fig. 10 with Fig. 2 demonstrates the reduction in amplitude of the betatron oscillations in the Main Ring by using this technique.

If desired, the small residual Main Ring oscillations can be eliminated totally by ramping the F46 and B13 bump magnets. Figure 11 shows an example of a stable orbit which is smooth in both the sector and the Main Ring with the exception of the local bumps at the Lambertson magnets.

Conventional Magnets in the Sector

In order to simplify the hot-cold transition between the superconducting Doubler and the conventional Main Ring for the purposes of the sector test, the superconducting magnets only run between A12 and A48. This means that the so-called structure quads at A11 and A49 together with the adjacent half cells will be made with conventional magnets. Because of space limitations on the allowable size of these magnets and power supply limitations, Main Ring magnets are not practically suitable for this task.

The available magnets suitable for the sector test include a selection of EPB dipoles and quads as well as some CEA quads. Replacing a given quad with one of a different length while maintaining the lattice, requires, in the zeroth order, the quad current to be scaled in such a fashion as to keep the $\int \frac{dB}{dx} \cdot \ell$ constant. A small first order correction to this value is then applied to take account of the change in length.

A complete lattice matching is not necessary and the elements shown together with the appropriate field values introduce a relative phase change of $\sim$0.008 across the replacement structure quads. These quads also possess a smaller effective aperture than the Main Ring quads ($\sim$2" vs. $\sim$4") and must be offset relative to the Main Ring to avoid seriously reducing the aperture. To avoid changing the lattice small horizontal steering magnets are required to cancel the effects of this offset. Appendicies II and III give the calculations on the positions and strengths of the steering magnets to achieve this offset cancellation.

The reduced length of the EPB dipoles together with the fact that a one for one duplication of the Main Ring bending magnets is not really necessary, require the EPB dipoles to be offset relative to the Main Ring. The standard

Doubler half cell itself has a small offset relative to the Main Ring which must be taken into account too. Appendix IV shows the calculations on EPB dipole positions relative to the Main Ring.

Tables IIA and IIB give the positions and field strength of the conventional magnets in the sector. It is worth noting at this point that the two CEA quads in Table IIB marked with an asterisk are replacing one 7-foot Main Ring quad and consequently the nominal field gradient in each one is set to 1/2 the value of $\int \frac{dB}{dx} \cdot \ell$ of the corresponding Main Ring quad.

Orbit Stability

Any question involving orbit stability of a circulating beam through the sector reduces immediately to the behaviour of the beam position at the Lambertson magnets. The reason is that the Lambertson magnets are located at relatively high beta values of the lattice and possess a horizontal aperture of $\sim$3 cms, smaller than any other element in the machine.

Figure 12 shows a graph of machine tune vs ramp time for a 400 GeV cycle selected at random. At 100 GeV the tune is starting to stabilize at 19.4 with a maximum excursion about the mean of $\lesssim$0.005. The momentum spreader in the Main Ring is also able to induce tune changes of this order of magnitude. To evaluate the effect of tune shifts of this size on the stable orbit through the sector, we scaled the Main Ring quad current to give the required tune change and looked at the beam position change while leaving the transfer system elements set to their nominal 19.31 values. The results are summarized below

| Tune | $\Delta x_1$ mm | $\Delta x_2$ mm | Tune | $\Delta x_1$ mm | $\Delta x_2$ mm |
|---|---|---|---|---|---|
| 19.26 | ±1.9 | ±2.1 | 19.32 | ±0.3 | ±0.5 |
| 19.28 | ±1.0 | ±1.4 | 19.34 | ±1.1 | ±1.3 |
| 19.30 | ±0.2 | ±0.3 | 19.38 | ±1.7 | ±2.0 |
| 19.31 | 0.0 | 0.0 | | | |

where $\Delta x_1$ and $\Delta x_2$ refer to the orbit displacements at the upstream and downstream Lambertsons respectively.

The results indicate that the small tune shifts expected in normal machine operation would not present any major problems from the point of view of phase space dilution.

Another important operational parameter for the sector test is momentum dispersion of the beam. Recent studies by the Main Ring Group yield a value for $\frac{\Delta p}{p}$ of $\sim 6.0 \times 10^{-4}$ for a beam energy of 100 GeV. A momentum spread of this value would give an increase in beam size of $1.0 \sim 2.0$ mm at the Lambertson magnets.

An estimate of the inherent beam spot size can be made from the horizontal transverse phase space area. At injection time from the booster (8.9 GeV) the area of the transverse phase space is taken to be $1.2\pi \times 10^{-6}$ mrad. At 100 GeV the area (90%) is given by

$$A_{100} = f \; \frac{8.9}{100} \; A_{8.9}$$

where f represents a phase space dilution factor. Setting f = 1 is equivalent to no phase space dilution and represents a lower bound on the area

$$\therefore A_{100}^{min} = 0.11\pi \times 10^{-6} \text{ mrad.}$$

A similar calculation scaling down from 400 GeV and setting f = 1 provides an upper bound on the area and yields

$$\therefore A_{100}^{max} = 0.2\pi \times 10^{-6} \text{ mrad.}$$

The beam spot size $\Delta x$ is related to A by

$$\Delta x = \pm \sqrt{A/\pi} \sqrt{\beta}$$

where $\beta$ is the beta value of the lattice at the position in question.

At the B0 Lambertson magnets $\beta_{max} \simeq 110$ m corresponding to

$$\Delta x_{max} \simeq \pm 4.7 \text{ mm}$$

$$\Delta x_{min} \simeq \pm 3.6 \text{ mm.}$$

A direct measurement on the beam using the internal beam sensor gives a value of ±4.0 mm in good agreement with this estimate.

In order to provide some feeling for the effect of replacing 1/6 of the Main Ring with the sector (which has a similar but non-identical lattice), the current Doubler lattice (D. E. Johnson based on TM-678 from T. Collins) has been incorporated into the computer simulation of the sector test. The results of this mismatch of the lattice show a $\frac{\Delta\beta}{\beta}$ value of $\sim$2% which varies sinusoidally around the ring. Lattice changes of this magnitude give rise to orbit changes of $\lesssim$1.0 mm. Consideration of the effect on stopband widths due to these lattice changes has not yet been attempted.

Conclusions

A first look at the main characteristics of the proposed sector test has not unearthed any major problems in the basic design. The establishment of a circulating beam through the sector is a complex problem in machine dynamics (a 3 cm Lambertson aperture with a 1 cm beam spot does not leave much room for error, especially in the case of multiple tranversals) and further study is required on such topics as stopband width in the "hybrid" machine, different tune and bend strength in the sector, and the effect of the rf system on the sort of orbits discussed in this report.

Fig 1.

TUNE 19.31
MAX.RADIAL OFFSET(CMS) 2.02
HORIZONTAL PROJECTION

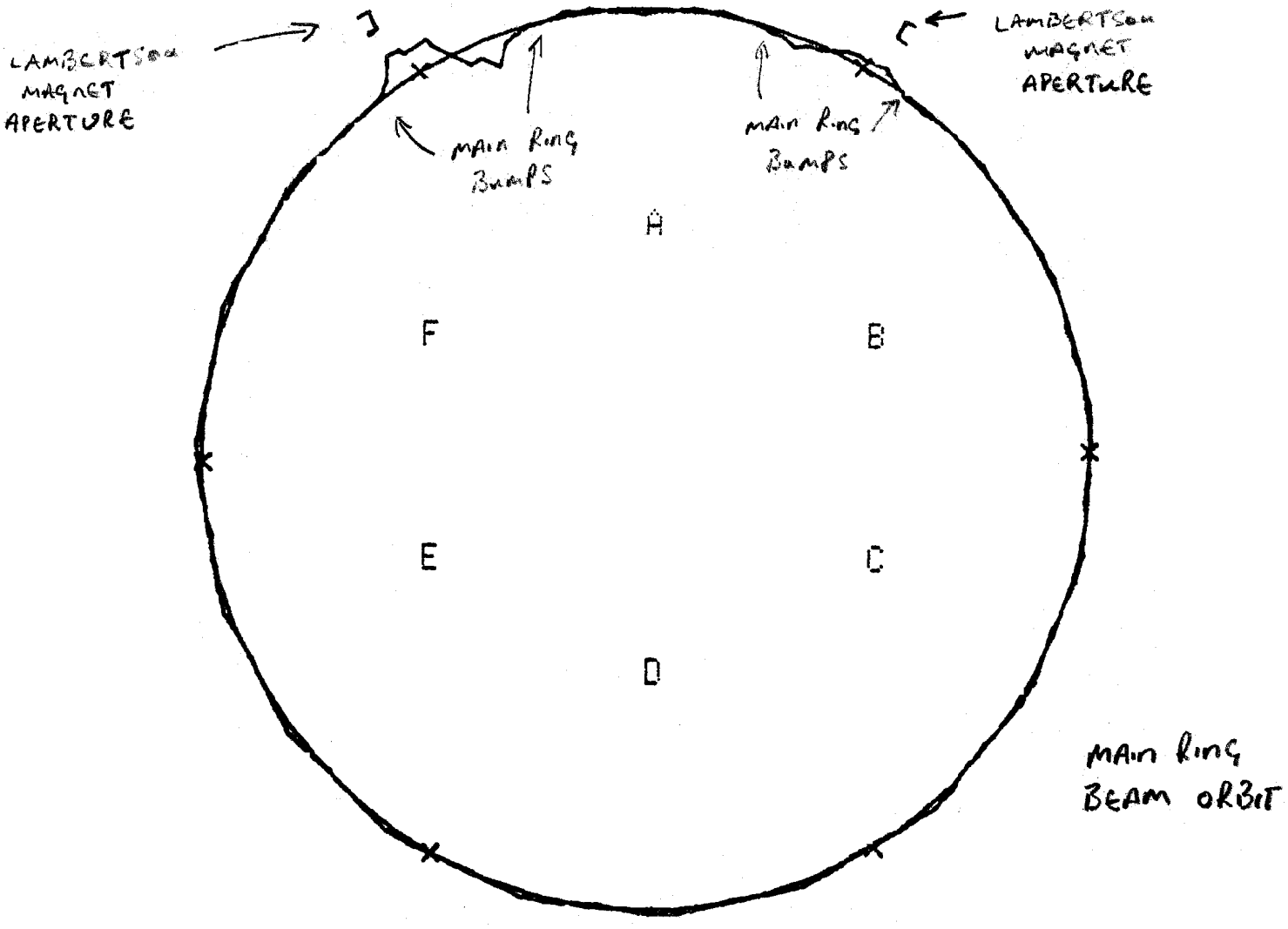


TM-785

TUNE 19.31
MAX.RADIAL OFFSET(CMS) 4.75
HORIZONTAL PROJECTION

Fig. 2

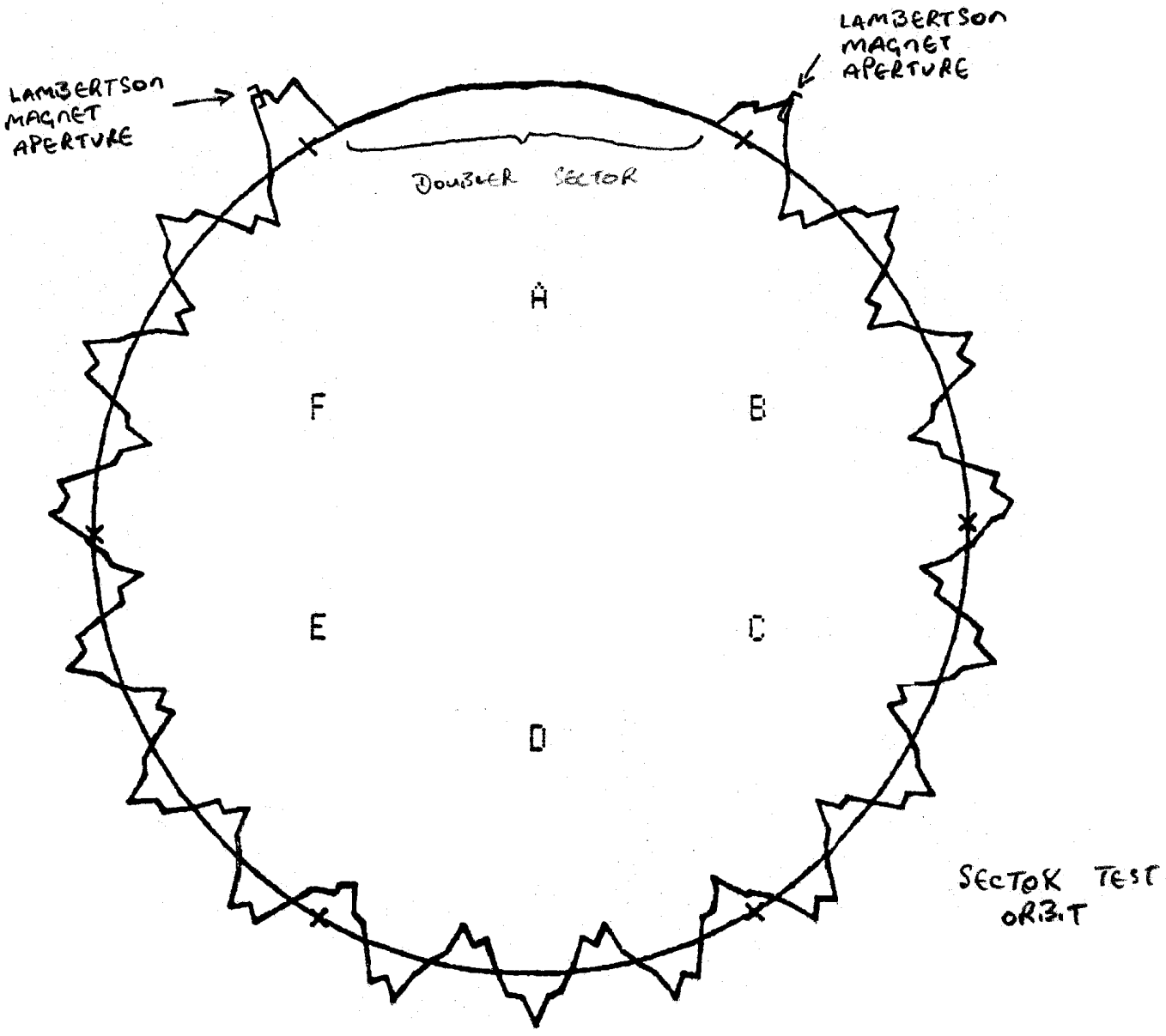

FIG 3 - BEAM POSITION AT LAMBERTSON MAGNET.
TRANSVERSE SECTION

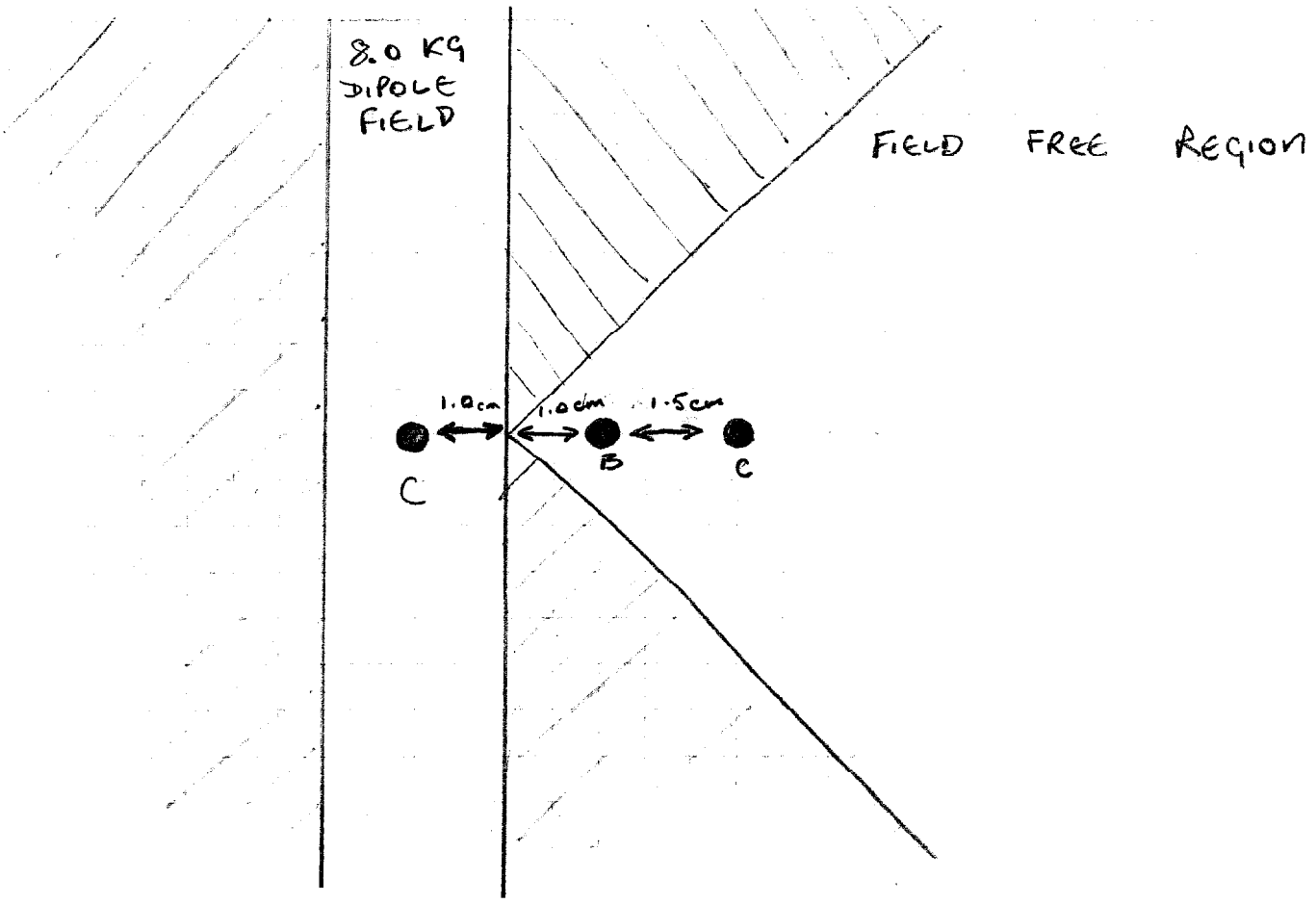


A - main ring stable orbit

B - stable orbit + local bump (c.f fig 1)

C - stable orbit + local bump + kicker (≡ stable sector orbit c.f. fig 2)

Beam spot size ~ ±4.5 mm at 100 GeV

TUNE 19.31
MAX.RADIAL OFFSET(CMS) 3.26
HORIZONTAL PROJECTION

Fig. 4

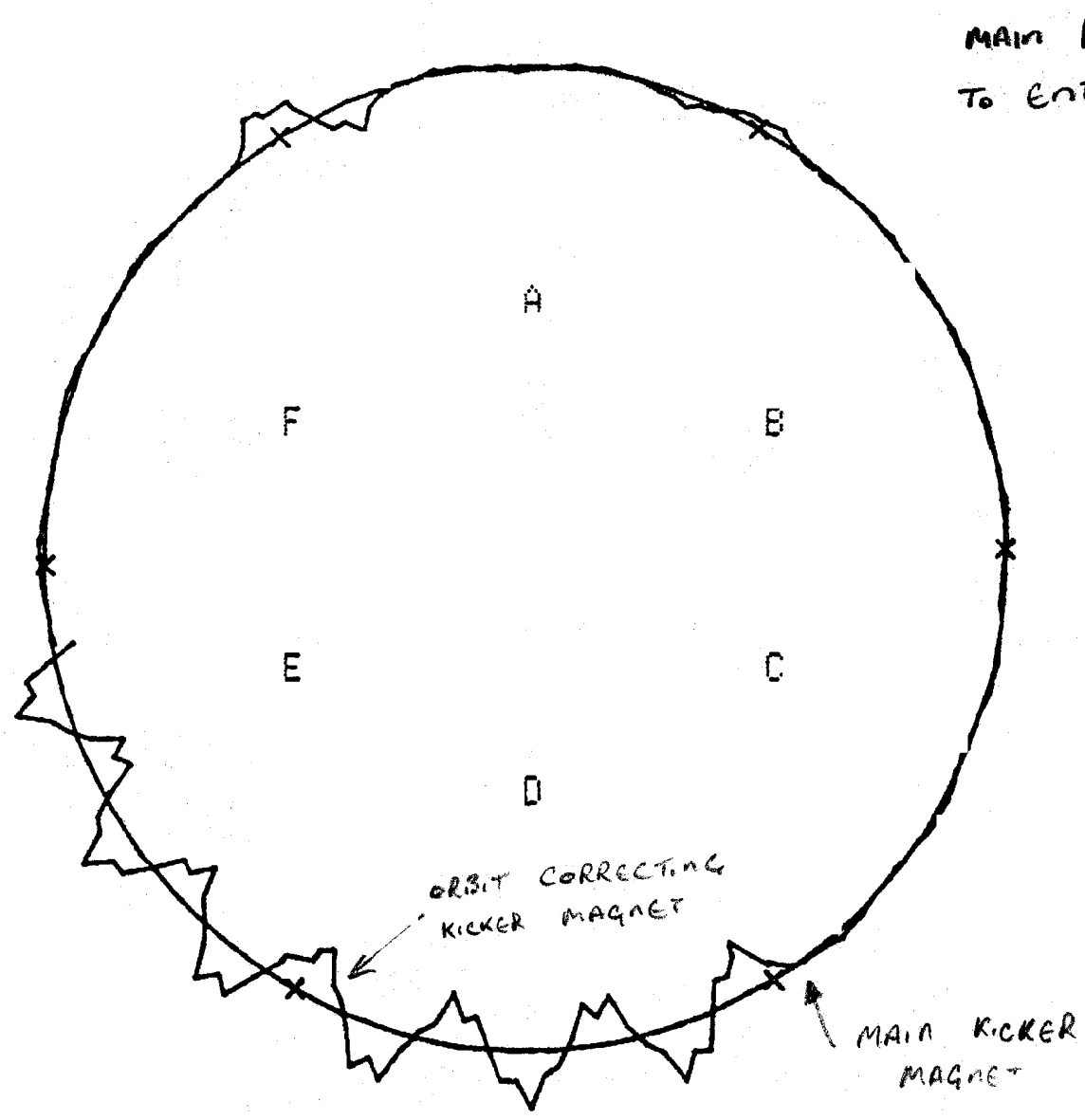

SECTOR TEST UPSTREAM DOGLEG (VERTICAL SECTION)

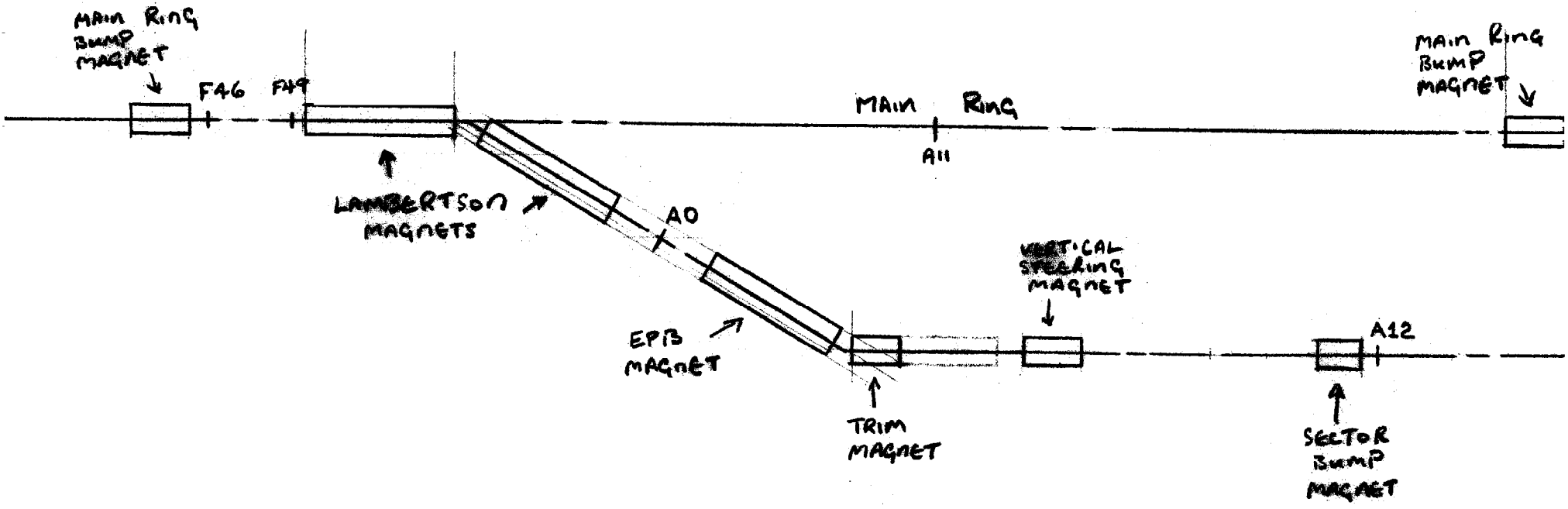


n.b. ONLY TRANSFER SYSTEM ELEMENTS SHOWN

FIG. 5

SECTOR TEST DOWNSTREAM DOGLEG (VERTICAL SECTION)

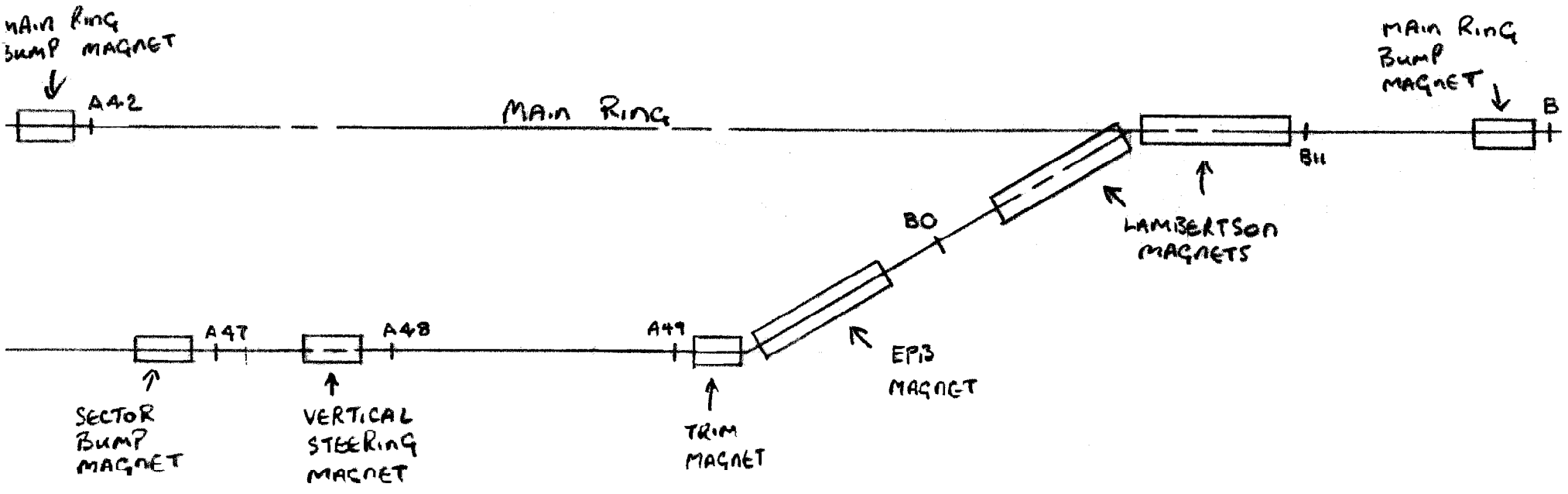


n.b. ONLY TRANSFER SYSTEM ELEMENTS SHOWN

FIG. 6

TUNE 19.400
MAX RADIAL OFFSET(CMS) 5.04
HORIZONTAL PROJECTION

SECTOR TEST ORBIT

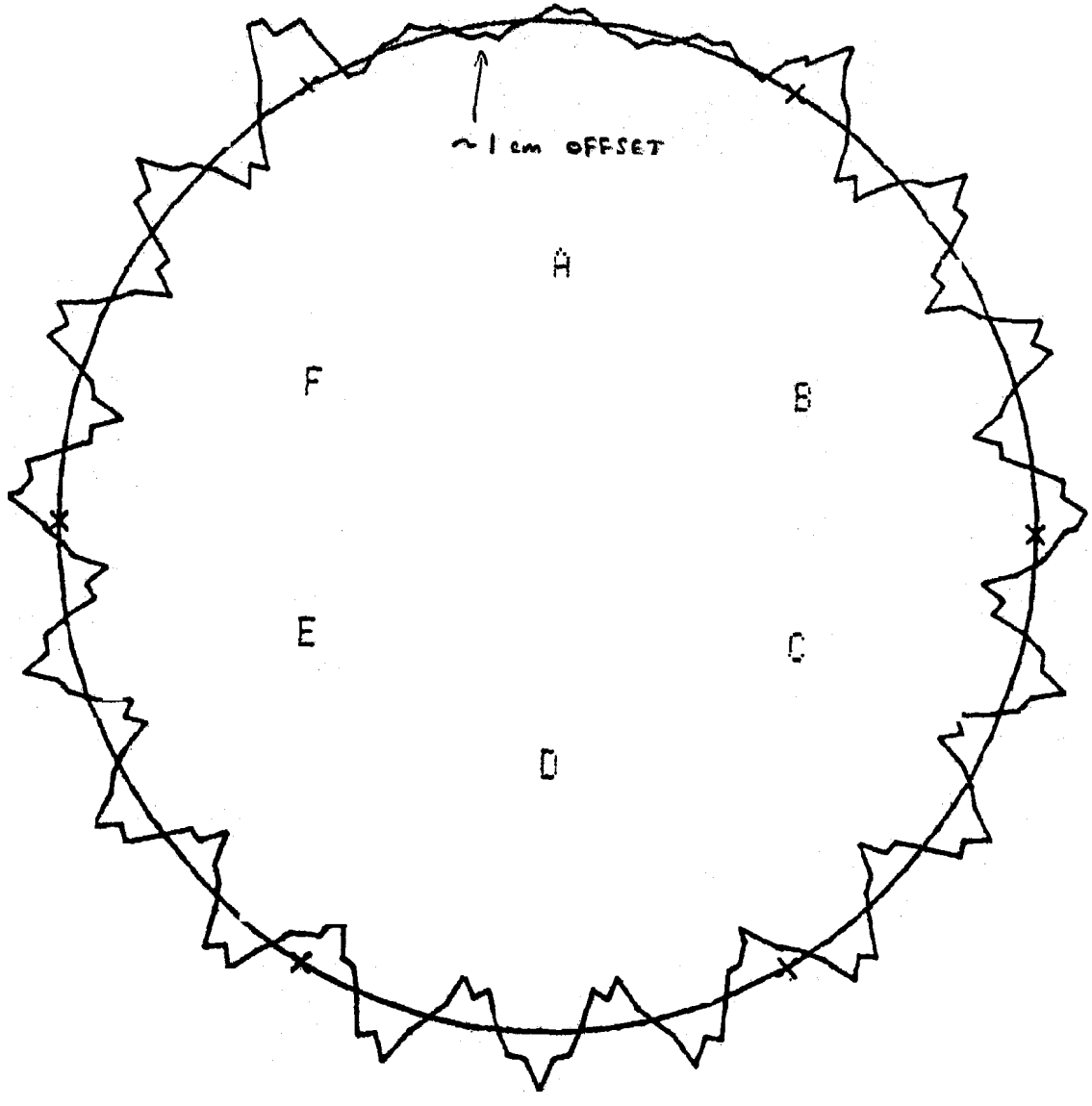

Fig. 8

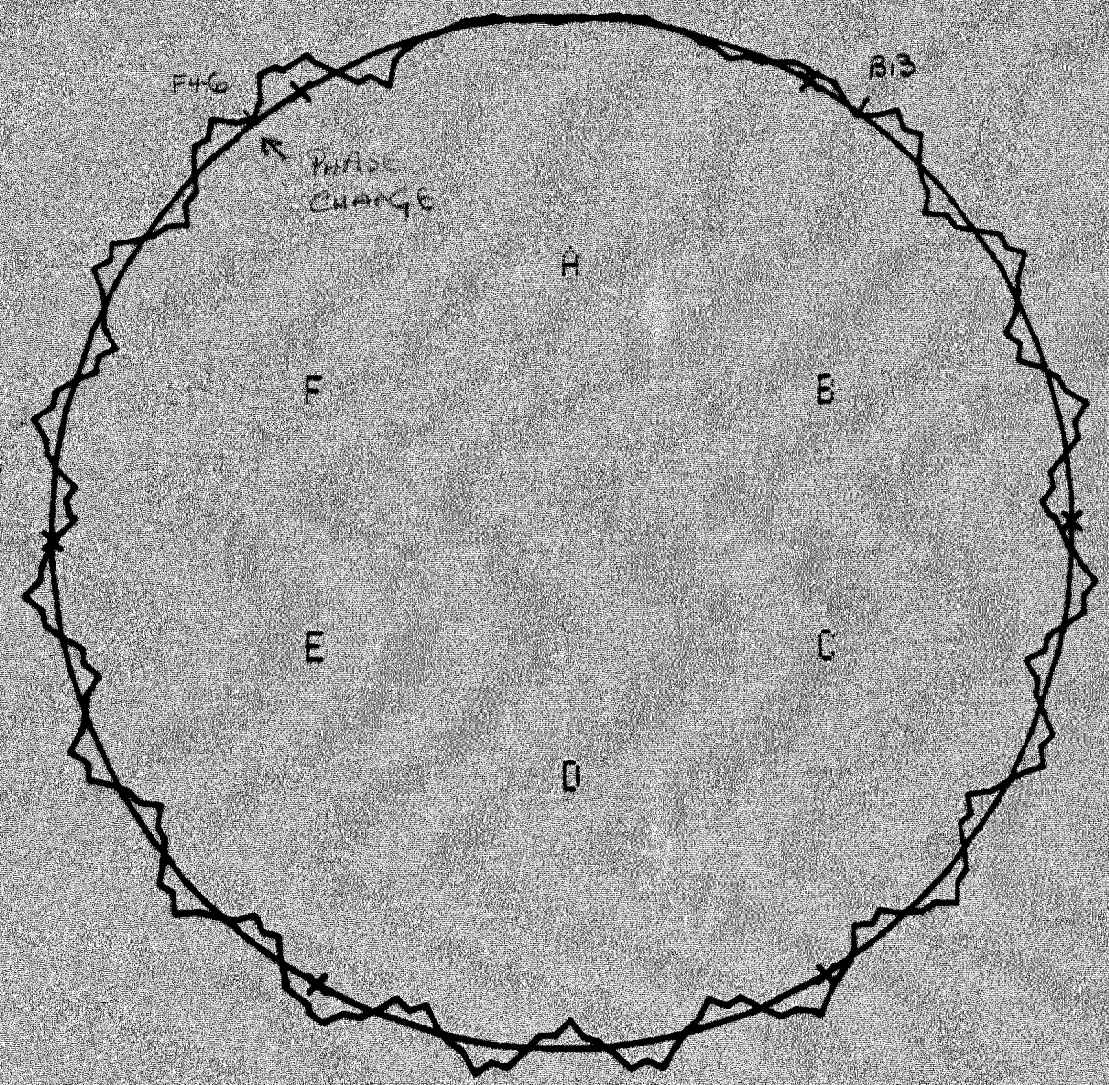
TUNE 19.310
MAX.RADIAL OFFSET(CMS) 2.03
HORIZONTAL PROJECTION
Main Ring ORBIT
F4G
B13
PHASE CHANGE
A
B
C
D
E
F

FIG. 9

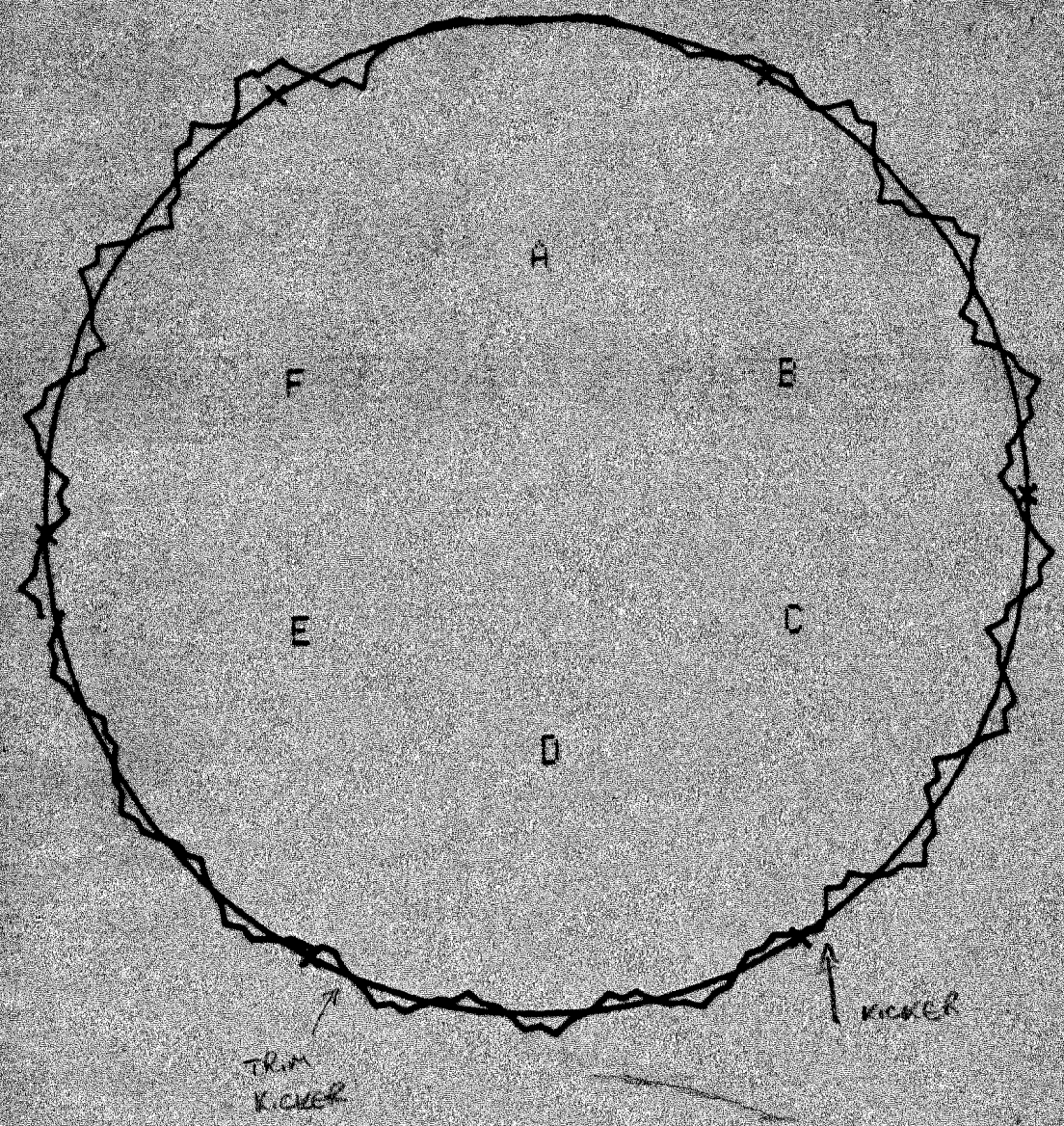


MAIN RING ORBIT PRIOR TO ENTERING SECTOR

Fig. 10

TUNE 19.310
MAX.RADIAL OFFSET(CMS) 4.51
HORIZONTAL PROJECTION

SECTOR TEST
ORBIT

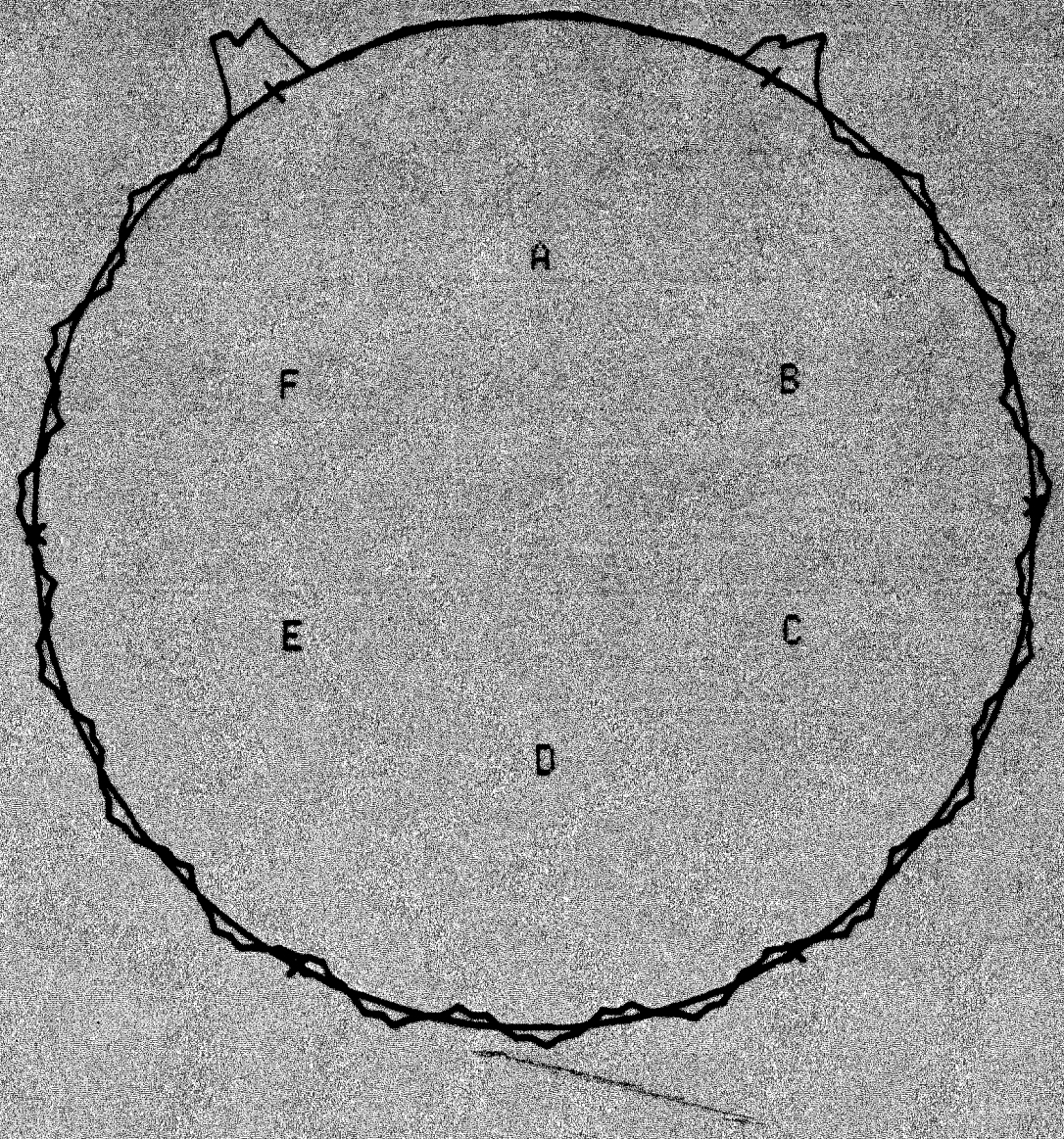

FIG. 11

TIME 19 310
MAX. RADIAL OFFSET(CMS) 4.71
HORIZONTAL PROJECTION

SECTOR TEST ORBIT

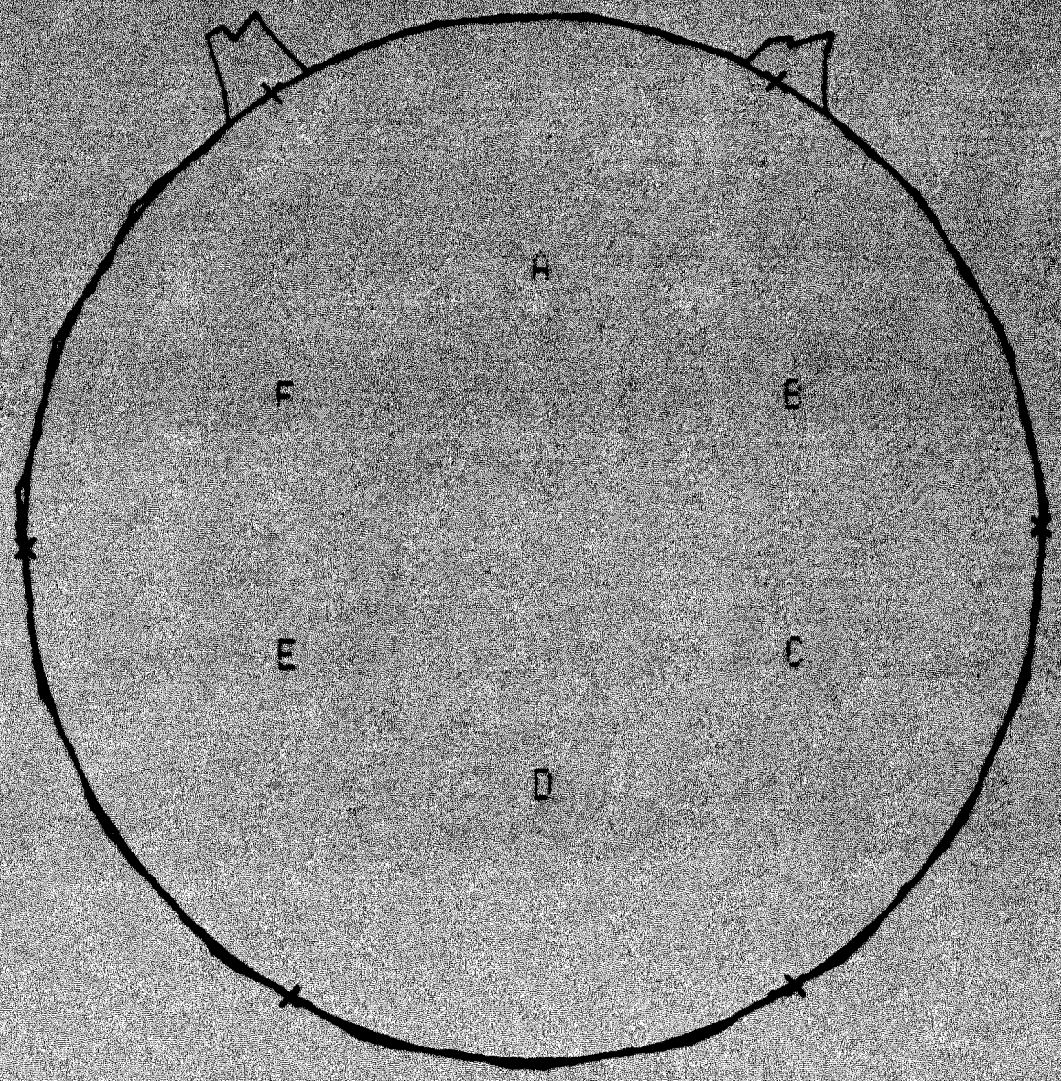

Fig. 12

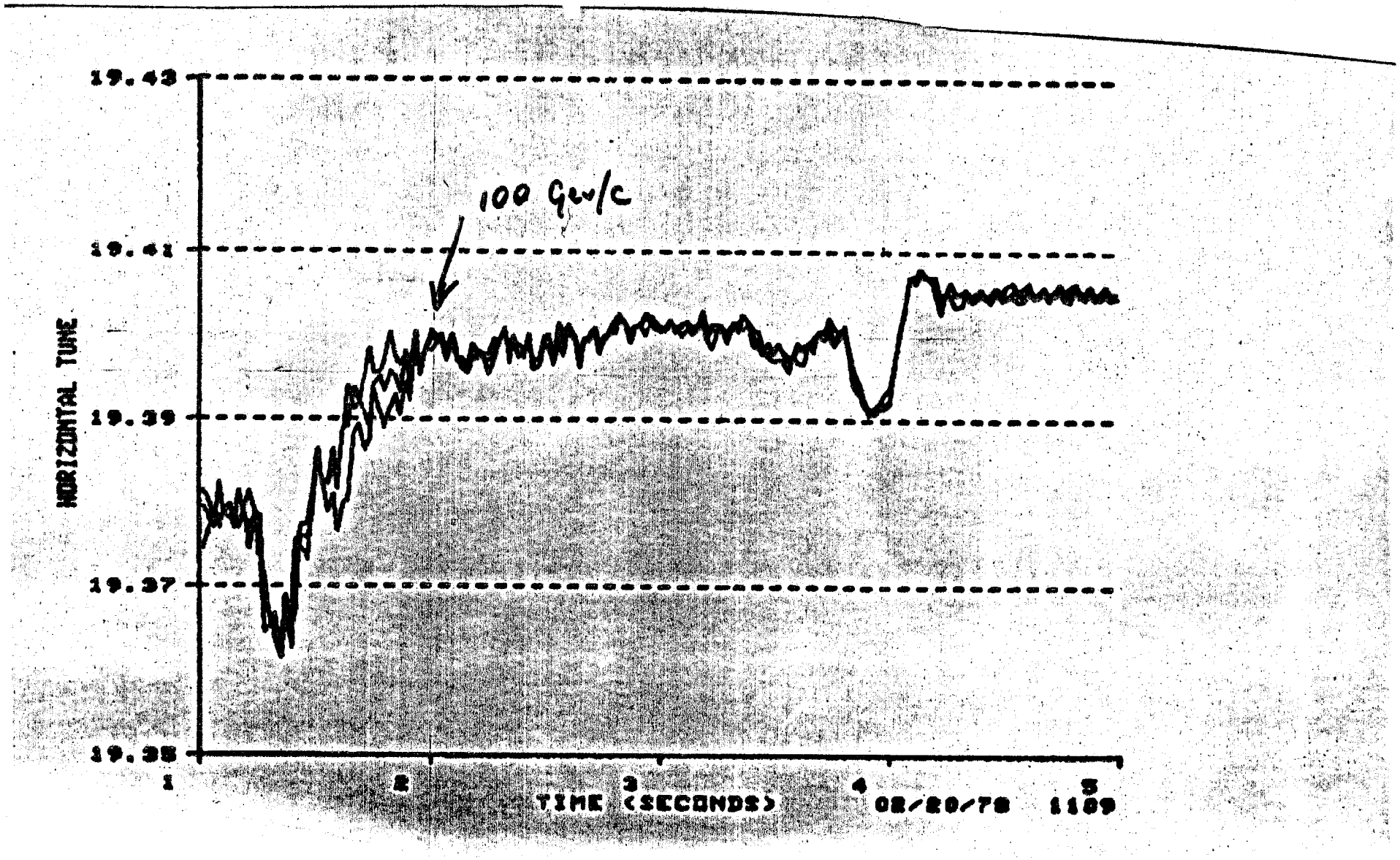
19.43
19.41
19.39
19.37
19.35
HORIZONTAL TUNE
100 GeV/c
1
2
3
4
5
TIME (SECONDS)
02/20/78
1109

TABLE I

| Element | Position (Element Centre) | Vertical Offset cms | Horizontal Offset cms | Bend Angle |
|---|---|---|---|---|
| Kicker | C48 Main Ring | 0.0 | 0.0 | -310 μR |
| Correcting Kicker | D48 Main Ring | 0.0 | 0.0 | 27 μR |
| Bump Horiz. | F46 Main Ring | 0.0 | 0.0 | 200 μR |
| Bump Horiz. | A17 Main Ring | 0.0 | 0.0 | -200 μR |
| Bump Horiz. | A42 Main Ring | 0.0 | 0.0 | - 50 μR |
| Bump Horiz. | B13 Main Ring | 0.0 | 0.0 | 50 μR |
| Bump Horiz. | 10' Upstream of Quad A12 Sector | -63.5 | 0.0 | 900 μR |
| BumP Horiz.* | A47 Sector | -63.5 | 0.0 | 650 μR |
| Lambertson** | A0 -23.4478 m Main Ring | 0.0 | -2.54 | - 7.5 mR |
| Lambertson** | A0 -19.8918 m Main Ring | 0.0 | -2.54 | - 7.5 mR |
| Lambertson** | B0 +19.8918 m Main Ring | 0.0 | -2.54 | - 7.5 mR |
| Lambertson** | B0 +23.4478 m Main Ring | 0.0 | -2.54 | - 7.5 mR |
| EPB Dipole | A0 +20.496 m Sector | -63.25 | -4.19 | 13.9 mR |
| Vertical Trim Dipole | A0 +22.782 m | -63.5 | -4.19 | 1.1 mR |
| Vert. Steering Magnet | A0 +58.83 m | -63.5 | 0.0 | ±800 μR |
| Vert. Steering Magnet | A49 -19.869 m | -63.5 | 0.0 | ±800 μR |
| Vertical Trim Dipole | B0 -22.782 m | -63.5 | +2.0 | 1.1 mR |
| EPB Dipole | B0 -20.496 m | -63.25 | +2.0 | 13.9 mR |

All horizontal and vertical offsets are relative to the Main Ring equilibrium orbit, as are bend angles. The coordinate system is right-handed with positive X radially outwards.

* Superconducting

**Lambertson offset measured to magnet septum.

TABLE IIA - CONVENTIONAL MAGNET PLACEMENT IN SECTOR

A0 ⟶ A12

| Magnet | Position (To Element Centre) | Horizontal Offset (cms) | Vertical Offset (cms) | Bend Angle (mr) | Correction Factor to $\int \frac{dB}{dx} \cdot \ell$ | Length m |
|---|---|---|---|---|---|---|
| Horizontal Steering Dipole | A0 + 18.035 | +3.94 | -59.55 | 0.480 | -- | 1.016 |
| EPB Quad | A11 - 3.5389 | +2.54 | -63.5 | -- | 0.99 | 1.397 |
| EPB Quad | A11 - 1.5413 | +2.54 | -63.5 | -- | 0.99 | 0.870 |
| EPB Quad | A11 + 1.5518 | +2.54 | -63.5 | -- | 0.99 | 0.870 |
| EPB Quad | A11 + 3.2169 | +2.54 | -63.5 | -- | 0.99 | 0.870 |
| EPB Dipole | A11 + 16.045 | +6.48 +8.27 | -63.5 | 10.82 | -- | 3.048 |
| EPB Dipole | A11 + 19.398 | +8.24 +8.08 | -63.5 | 10.82 | -- | 3.048 |
| EPB Dipole | A11 + 22.750 | +8.05 +5.81 | -63.5 | 10.82 | -- | 3.048 |
| EPB Quad | A12 - 0.8097 | 0.356 | -63.5 | -- | 0.99 | 0.870 |

TABLE IIB - CONVENTIONAL MAGNET PLACEMENT IN SECTOR

A48 ⟶ BO

| Magnet | Position (To Element Centre) | Horizontal Offset (cms) | Vertical Offset (cms) | Bend Angle (mr) | Correction Factor to $\int \frac{dB}{dx} \cdot \ell$ | Length m |
|---|---|---|---|---|---|---|
| Cornell Quad | A48 - 1.628 | 0.356 | -63.5 | -- | 0.96 | 0.508 |
| EPB Dipole | A49 - 15.268 | 5.05<br>6.52 | -63.5 | 12.18<br>+0.1 | -- | 3.048 |
| EPB Dipole | A49 - 11.916 | 6.50<br>5.22 | -63.5 | 12.18<br>+0.1 | -- | 3.048 |
| Cornell Quad | A49 - 3.217 | 2.54 | -63.5 | -- | 0.96 | 0.508 |
| Cornell Quad | A49 - 1.551 | 2.54 | -63.5 | -- | 0.96 | 0.508 |
| Cornell Quad | A49 + 1.541 | 2.54 | -63.5 | -- | 0.96 | 0.508 |
| Cornell* Quad | A49 + 3.088 | 2.54 | -63.5 | -- | 0.96 | 0.508 |
| Cornell* Quad | A49 + 3.988 | 2.54 | -63.5 | -- | 0.96 | 0.508 |
| Horizontal Steering Magnet | BO - 18.061 | 2.0 | -59.6 | 0.346 | -- | 1.016 |

## APPENDIX 1 - Local Machine Orbit Distortions

Generating local distortions in the Main Ring orbit is accomplished by using a small "bump" dipole magnet to generate a betatron oscillation and then a second bump magnet to remove the oscillation created by the first one. Schematically the situation looks like

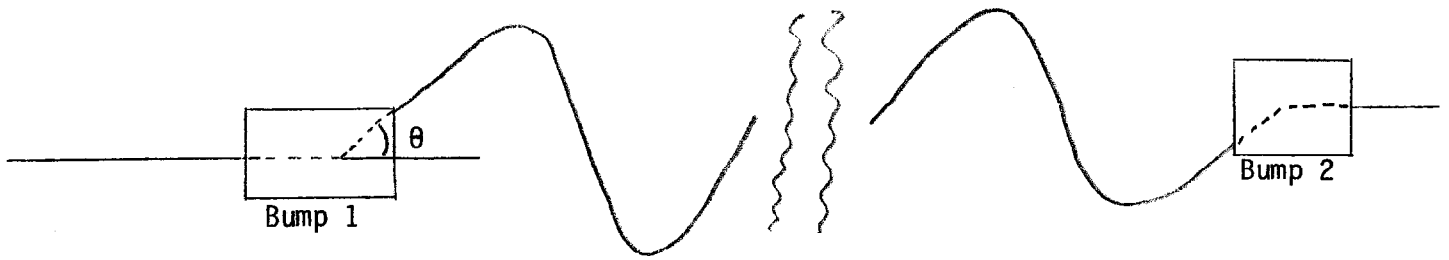


In order to cancel the betatron oscillation exactly the magnet positions in the lattice and the machine tune must conspire to produce a relative phase advance of $n\pi$ (where n is an integer) between the two magnets. If we impose the further condition that the magnitude of the bend angles in each magnet be equal (i.e. a single power supply) then the values of $\beta$ (betatron oscillation wavelength) at both magnets must be the same.

In practice these ideal conditions are never completely realized. The local orbit distortion around A0 in the sector test for example has the following parameters:

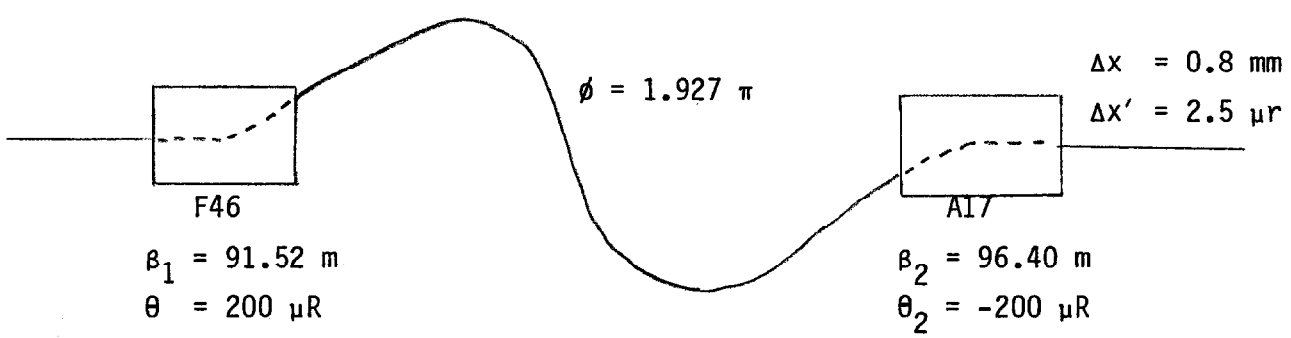

## APPENDIX II - Structure Quad Offset at A11

The induced betatron oscillations in the ring at injection into the sector create an offset in beam position of $\sim$4.0 cms at A11. The EPB quads used in the lattice at this point have an effective apperture of $\sim\pm$3.8 cms and consequently would obstruct the beam if positioned directly beneath the Main Ring. The solution to this problem is to offset the EPB quads relative to the Main Ring and then cancel out the lattice distortion this offset produces with a horizontal dipole. The position and strength of this dipole being determined by the required offset of the quads.

The beam transfer matrix from the (as yet undetermined position of the) dipole to the far end of the quads can be written as

$$\begin{pmatrix} x_1 \\ x_1' \end{pmatrix} = \begin{pmatrix} 1 & \ell \\ 0 & 1 \end{pmatrix} \begin{pmatrix} A & B \\ C & D \end{pmatrix} \begin{pmatrix} X \\ X' \end{pmatrix}$$

where $\ell \equiv$ drift length from the dipole to the quads

$\begin{matrix} A & B \\ C & D \end{matrix}$ $\equiv$ the transfer matrix through the quads.

$x, x'$ $\equiv$ the position and angle of the beam.

If we now displace the quads a distance $\Delta_x$ and give the dipole a kick of $\theta$ and require the orbit to be unchanged we have

$$\begin{pmatrix} x_1 - \Delta_x \\ x_1' \end{pmatrix} = \begin{pmatrix} 1 & \ell \\ 0 & 1 \end{pmatrix} \begin{pmatrix} A & B \\ C & D \end{pmatrix} \begin{pmatrix} X - \Delta_x \\ x' + \theta \end{pmatrix}$$

solving between these two equations we obtain

$$\ell = \frac{DA-BC-D}{C} \qquad \theta = \frac{C\Delta_x}{C\ell+D} .$$

For a tune of 19.31 the transfer matrix through the quad gives

$$\begin{pmatrix} A & B \\ C & D \end{pmatrix} \equiv \begin{pmatrix} 0.6312 & 9.6399 \\ -0.0258 & 1.1902 \end{pmatrix}$$

which gives

$$\ell = -7.379 \text{ m} \quad (\longrightarrow \text{A0} + 18.035)$$

defining the quad offset to be 2.54 cms, then

$$\theta = 0.480 \text{ ms.}$$

## APPENDIX III - Structure Quad Offset at A49

A similar problem to that discussed in Appendix I also exists at A49. Solving the problem in a similar fashion gives a physically inappropriate solution, i.e. correction dipole ∿150 m downstream of B0 (not a nice place to put a dipole). To provide a more realistic position for this dipole, a double bump solution is necessary. The first bump comes from running the two EPB dipoles in the A48 - A49 half cell to give at kick 0.1 mr greater than that required by the Main Ring lattice. This is equivalent to having a bump magnet of strength 0.2 mr positioned between the two dipoles.

Using similar logic to Appendix I the equations to solve are:

$$\begin{pmatrix} x_1 \\ x_1' \end{pmatrix} = \begin{pmatrix} 1 & \ell \\ 0 & 1 \end{pmatrix} \begin{pmatrix} A & B \\ C & D \end{pmatrix} \begin{pmatrix} x \\ x' \end{pmatrix}$$

where $\ell$ = drift length from the quads to the correction dipole.

$\begin{pmatrix} A & B \\ C & D \end{pmatrix}$ = The transfer matrix from the centre of the EPB dipoles to the downstream end of the quads.

and

$$\begin{pmatrix} x_1 - \Delta_x \\ x_1' - \theta_2 \end{pmatrix} = \begin{pmatrix} 1 & \ell \\ 0 & 1 \end{pmatrix} \begin{pmatrix} A & B \\ C & D \end{pmatrix} \begin{pmatrix} x - \Delta_x \\ x' - \theta_1 \end{pmatrix}$$

where $\Delta_x$ = quad offset

$\theta_1$ = effective kick from the EPB dipoles

$\theta_2$ = required kick from the correction dipole

solving for $\ell$ and $\theta_2$ we get

$$\ell = \frac{-B\theta_1 + \Delta_x(1-A)}{C\Delta_x + D\theta_1}, \quad \theta_2 = C\Delta_x + D\theta_2$$

using $\Delta_x$ = 2.54 cms, $\theta_1$ = -0.2 mr

and $$\begin{pmatrix} A & B \\ C & D \end{pmatrix} \equiv \begin{pmatrix} 0.7688 & 16.6215 \\ 0.0029 & 1.3637 \end{pmatrix}$$

we get

$$\ell = 7.356 \text{ m } (\longrightarrow \text{BO} - 18.061 \text{ m})$$

$$\theta_2 = 0.346 \text{ mr.}$$

## APPENDIX IV - EPB Dipole Position Relative to the Main Ring A11→A12, A48→A49

The sector test calls for replacing 4 Main Ring bending magnets with 3 EPB dipoles in the A11-A12 section. THe EPB dipoles will require a radial offset from the beam position to compensate for the different geometry. This radial offset can be thought of as being made up of several components.

i) Doubler offset - the ends of each half cell in the Doubler lattice are 0.356 cms radially out from the equivalent Main Ring positions

ii) Betatron offset - the Main Ring betatron oscillations have not yet been removed at this point in the sector

iii) Sagitta offset - the different lengths and fields in the EPB dipoles give rise to a different sagitta inside the magnet.

The sagitta in a bending magnet is calculated as follows:

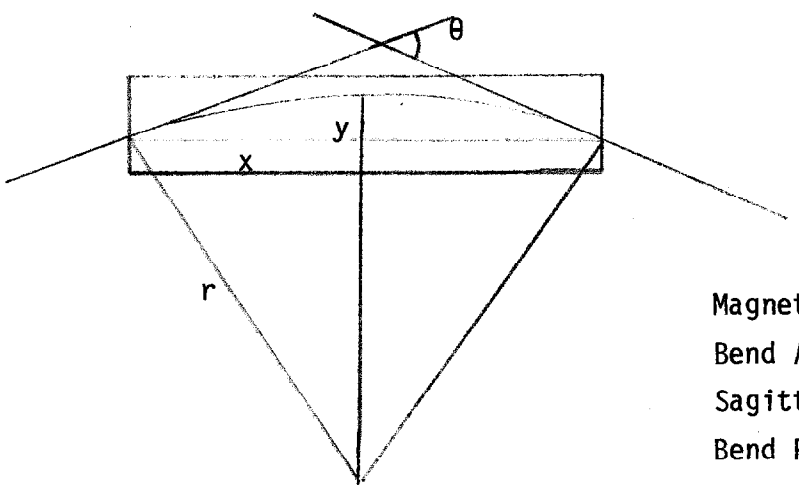


Magnet Length = 2x
Bend Angle = θ
Sagitta = y
Bend Radius = r

$y = r(1-\cos\theta/2)$

$r = x/\sin\theta/2 \quad > \quad 4 = x(1-\cos\theta/2)/\sin\theta/2$

for an EPB magnet $x = 152.4$ cms $\theta = 10.82$ mr

$\longrightarrow$ $y = 0.412$ cms

Main Ring dipole $x = 303.53$ $\theta = 8.12$ mr

$\longrightarrow$ $y = 0.61$ cms.

iv) Chord offset - the different geometry of the half cell mean that the beam trajectory will follow a different arc on a chord of fixed length.

We consider the general case of n dipoles of a given length $\ell$ and bend angle $2\theta$. Each dipole is separated by a gap G. There are two drift lengths at the start and end of the half cell of lengths E and F. These parameters then define the problem. The results we require are the magnet offsets from the chord at both ends of each magnet. Schematically the problem is as follows:

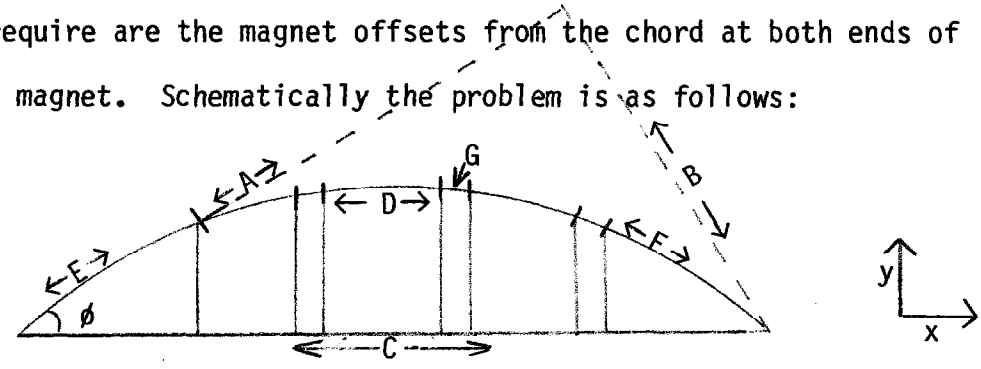


Radius of curvature in magnet $R = \ell/2\theta$

define $R' = (\ell+G)/2\theta$

where $R'$ is an effective radius of curvature ($\ell \gg G$)

then $D = 2R\sin\theta$

$A = E+2R' \sin 2n\theta+F\cos 2n\theta$

$B = R'(1-\cos 2n\theta)+F\sin 2n\theta$

$C = \sqrt{(A^2+B^2)}$

$\phi = \tan^{-1}(B/A)$